Journal of Quantitative Spectroscopy & Radiative Transfer 109 (2008) 2376–2385

Contents lists available at ScienceDirect

Journal of Quantitative Spectroscopy & Radiative Transfer

journal homepage: www.elsevier.com/locate/jqsrt

Toward unified satellite climatology of aerosol properties: Direct comparisons of advanced level 2 aerosol products

Li Liu [a,b], Michael I. Mishchenko [a,*]

[a] NASA Goddard Institute for Space Studies, 2880 Broadway, New York, NY 10025, USA
[b] Columbia University, 2880 Broadway, New York, NY 10025, USA

ARTICLE INFO

Article history:
Received 15 April 2008
Received in revised form
2 May 2008
Accepted 6 May 2008

Keywords:
Tropospheric aerosols
Remote sensing

ABSTRACT

The development of a unified satellite climatology of aerosol properties requires accurate quantification and deep understanding of the underlying factors contributing to discrepancies between individual satellite products. In this paper we compare the most recent level 2 results obtained for coincident pixels viewed at essentially the same time by the Moderate Resolution Imaging Spectroradiometer (MODIS) and Multiangle Imaging Spectroradiometer (MISR) instruments flown on the EOS Terra platform. This strategy eliminates potential sampling effects and provides a virtually direct comparison of spatially and temporally collocated MODIS and MISR retrievals. We show that the MODIS and MISR Ångström exponent datasets reveal essentially no correlation. Although the corresponding aerosol optical thickness (AOT) datasets can agree worse than expected over the oceans, still the agreement is often satisfactory. However, the agreement over the land is often poor or even unacceptable. Of the collocated pixels for which there is a MODIS aerosol retrieval, only ~40% or fewer pixels have a MISR aerosol retrieval, and vice versa. These findings further illustrate the complexity of the problem of aerosol retrievals from satellite observations and indicate that the creation of a meaningful unified MODIS–MISR aerosol climatology will be a nontrivial task.

Published by Elsevier Ltd.

1. Introduction

Remote sensing from satellite platforms based on advanced radiative transfer and electromagnetic scattering models is the only way to gather continuous global information about the spatial and temporal distribution of tropospheric aerosols. With a nearly three-decade record, the aerosol product generated in the framework of the Global Aerosol Climatology Project (GACP) [1–5] provides valuable information on potential global and regional long-term aerosol trends over the oceans [6–8]. However, because the GACP algorithm is based only on channel-1 and -2 Advanced Very High Resolution Radiometer (AVHRR) radiances, it has an inherently limited retrieval capability and must rely on many a priori assumptions with regard to the numerous parameters of the atmosphere–surface system other than the aerosol optical thickness (AOT) and Ångström exponent (AE) [1]. The absence of an on-board radiance calibrator serves to further exacerbate the problem. The GACP AOT dataset has been calibrated versus ship-borne sun-photometer results [9,10]. However, it would be preferable to base a systematic global test and final tuning of the GACP retrieval algorithm on comparisons with potentially more advanced satellite aerosol products, e.g., the Moderate Resolution Imaging Spectroradiometer (MODIS) and Multiangle Imaging Spectroradiometer (MISR) datasets. Indeed, this could provide additional constraints on the a priori

* Corresponding author. Tel.: +1 212 678 5590; fax: +1 212 678 5552.
E-mail address: mmishchenko@giss.nasa.gov (M.I. Mishchenko).

0022-4073/$ - see front matter Published by Elsevier Ltd.
doi:10.1016/j.jqsrt.2008.05.003

assumptions used in the GACP retrieval algorithm and make them more realistic on the global scale. Of course this is also true of the standard NOAA aerosol product based on channel-1 AVHRR data [11,12].

Previous studies have indicated that global monthly averages of the MODIS and MISR AOTs differ systematically by about 0.03–0.05 [4,13], with MODIS producing generally higher mid-visible AOTs than MISR over land and MISR producing generally higher AOTs than MODIS over water (e.g., [14–17]). The likely contributors to the MODIS–MISR discrepancies include differences in absolute radiometric calibration, cloud screening, algorithm assumptions regarding aerosol microphysical and optical properties [18], and surface boundary conditions, as well as spatial sampling. Obviously, it would be problematic to give preference to either of these two aerosol datasets or to create an integrated MODIS–MISR product without deep understanding and accurate quantification of the underlying factors that contribute to the identified systematic discrepancies.

This overarching issue was articulated and discussed in our recent perspective [13]. In that paper we also made the first attempt to analyze this problem on the regional scale by comparing level 3 MODIS and MISR products. Somewhat unexpectedly, that comparison revealed substantial differences between regionally averaged MODIS and MISR AOTs, which significantly exceeded the individual MODIS and MISR pixel-level accuracy claims as well as the maximal tolerable levels of uncertainty dictated by the need to significantly improve our understanding of the direct and indirect effects of aerosols on climate [19,20].

An obvious shortcoming of that preliminary analysis is that its results could have been affected by MODIS–MISR sampling differences. Therefore, the strategy adopted for this sequel paper is to eliminate the potential sampling effects completely. To this end, we will compare level 2 results obtained only for coincident pixels viewed at exactly the same time by the MODIS and MISR instruments flown on the same EOS Terra platform. In other words, we will analyze only MODIS-Terra and MISR retrievals for collocated pixels within the significantly narrower MISR swath.

It should be noted that Kahn et al. [17] have recently published an in-depth analysis of selected MODIS and MISR AOT retrievals over dark ocean water. However, their focus was on five specific Aerosol Robotic Network (AERONET) locations and only on the days that were simultaneously declared cloud-free by the MODIS, MISR, and AERONET retrieval algorithms. In contrast, our comparison strategy is based on a systematic use of large volumes of collocated MODIS and MISR data and is expected to eventually yield a much better understanding of the strengths and limitations of the MODIS and MISR aerosol datasets and their utility in regional and global climate studies.

2. MODIS and MISR data

The MODIS-Terra instrument has a viewing swath width of 2330 km and covers the entire surface of the Earth every 1–2 days with a moderate spatial resolution (250–1000 m). Its detectors yield radiance measurements in 36 spectral bands ranging in wavelength from 400 to 14,400 nm, seven of which (nominal wavelengths 470, 550, 660, 870, 1240, 1640, and 2130 nm) are used to characterize aerosol optical properties. MODIS includes on-orbit calibration [21]. A detailed description of the aerosol-retrieval algorithm can be found in [22–24]. It has been claimed that one standard deviation of MODIS AOT retrievals fall within the predicted uncertainty of $\Delta(\mathrm{AOT}) = \pm 0.03 \pm 0.05 \times \mathrm{AOT}$ over ocean and $\Delta(\mathrm{AOT}) = \pm 0.05 \pm 0.15 \times \mathrm{AOT}$ over land, while one standard deviation of MODIS effective radius retrievals fall within $\Delta r_{\mathrm{eff}} = \pm 0.11\,\mu\mathrm{m}$ [24].

In this study, we use the recently released MODIS collection 5 level 2 aerosol products that are available from the NASA Goddard Space Flight Center's Atmosphere Archive and Distribution System (http://ladsweb.nascom.nasa.gov). The MODIS level 2 standard aerosol product reports AOT on a 10 km grid of 10×10 1-km pixels, along with the AE, effective radius, and fine mode fraction retrieved over both land and ocean. Each MODIS orbit is separated into 5-min chunks called "granules". The size of each granule is about 2030 km (about 203 scans of 10 km) along the orbital path.

The MISR instrument consists of nine pushbroom cameras that view the Earth in nine different directions (four forward, four backward, and nadir) at four wavelengths (446, 558, 672, and 866 nm) and also includes in-flight radiance calibration [25]. MISR has a 360-km-wide swath, taking 9 days for complete global coverage. The aerosol-retrieval methodologies used with MISR data have been described in [26,27]. It has been claimed that about 2/3 of the MISR AOT values fall within ± 0.05 or $\pm 0.2 \times \mathrm{AOT}$ of AERONET, while more than a third are within ± 0.03 or $\pm 0.1 \times \mathrm{AOT}$ [28].

The MISR product, downloadable through the NASA Langley Research Center's Atmospheric Sciences Data Center (http://eosweb.larc.nasa.gov), consists of the AOT, AE, and aerosol type retrieved over both land and ocean. MISR level 2 products are in swaths, each derived from a single MISR orbit, where the imagery is 360 km wide and approximately 20,000 km long. The MISR level 2 standard aerosol product reports the AOT and the other aerosol parameters on a 17.6 km grid of 16×16 1.1-km pixels.

We have downloaded and analyzed 2 full months of level 2 MODIS-Terra collection 5 and MISR version 18 aerosol data corresponding to January and July 2006. However, to save space the following discussion will be largely focused on January 2006 data. The data are written as scientific datasets (SDSs) in the HDF format. In what follows, unless mentioned otherwise, we refer to MODIS 10 km resolution or MISR 17.6 km resolution level 2 grids as pixels. The SDSs that we use in this study include the following.

For MODIS:

- Corrected_Optical_Depth_Land
- Angstrom_Exponent_Land

- Quality_Assurance_Land
- Cloud_Fraction_Land
- Effective_Optical_Depth_Average_Ocean
- Angstrom_Exponent_1_Ocean
- Quality_Assurance_Ocean
- Cloud_Fraction_Ocean

For MISR:

- RegBestEstimateSpectralOptDepth
- RegBestEstimateAngstromExponent
- RetrAppMask

3. Comparisons of January 2006 MODIS and MISR results

3.1. Global comparisons

Fig. 1 compares MODIS and MISR AOTs at a wavelength of 550 nm retrieved for coincident MODIS and MISR pixels over the land (left-hand panel) and the oceans (right-hand panel). All MODIS and MISR pixels are collocated to within 3.3 km and ~3 min. There is a total of 290,430 collocated MISR and MODIS pixels with retrieved AOT, of which 84,732 are over the land and 205,698 are over water surfaces. Of course, the total number of collocated MODIS and MISR pixels is much larger than 290,430, but the MODIS dataset, the MISR dataset, or both do not have aerosol-retrieval results over the remaining collocated pixels.

It can be seen that the MODIS–MISR differences are especially large over the land. The agreement between the two datasets is considerably better over the oceans, which is not surprising since the retrieval of aerosol properties over dark underlying surfaces is a much easier task [1]. The respective globally averaged AOTs over the oceans agree much better: 0.132 for MODIS and 0.138 for MISR. However, MODIS yields a much lower globally averaged AOT over the land, viz., 0.130 versus 0.174 for MISR. This result appears to disagree with some of the previous assessments, which can be due to our calculation of averages based on collocated pixels rather than the entire datasets, to our use of only 1 month of data, and/or due to our use of the most recent MODIS and MISR products. However, it does appear somewhat suspicious that the average MODIS AOTs over the land and over the oceans are virtually the same since one would typically expect the atmosphere to be cleaner over the oceans. Obviously, further studies are needed before drawing a definitive conclusion.

Fig. 2 compares MODIS and MISR AOTs at 550 nm over the oceans under different cloud conditions ranging from "perfectly clear" skies to cloud fractions over 80%. The cloud fraction data used here are taken from the MODIS retrieval results. The MODIS and MISR AOT retrievals agree significantly better when the cloud fraction is small. The linear correlation coefficient between the two datasets is 0.922 for cloud-free conditions and gradually decreases to 0.896, 0.884,

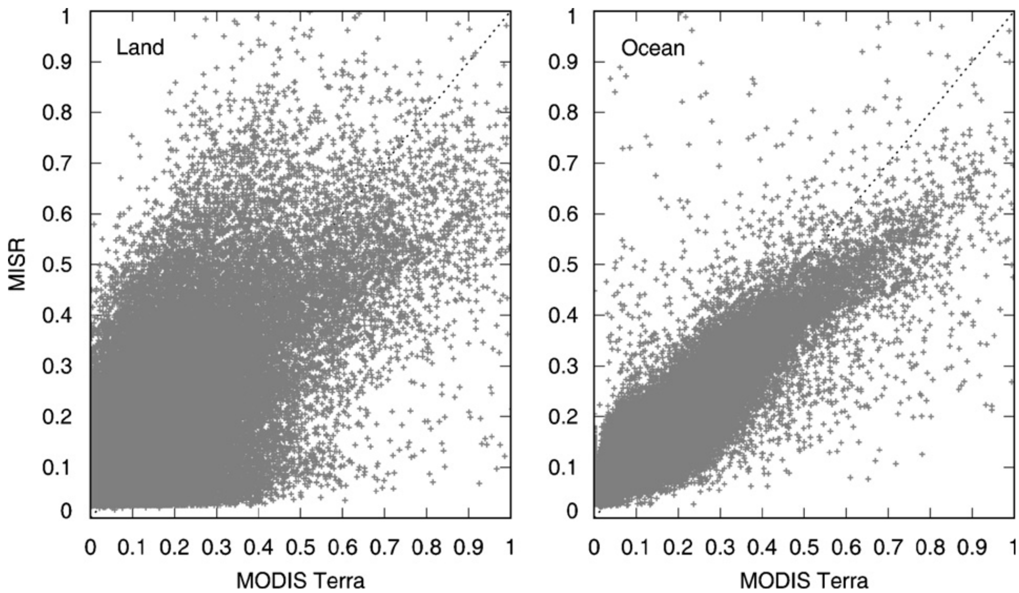

Fig. 1. Scatter plots of coincident MISR vs. MODIS-Terra AOTs for January 2006. The straight dotted line depicts the one-to-one perfect agreement.

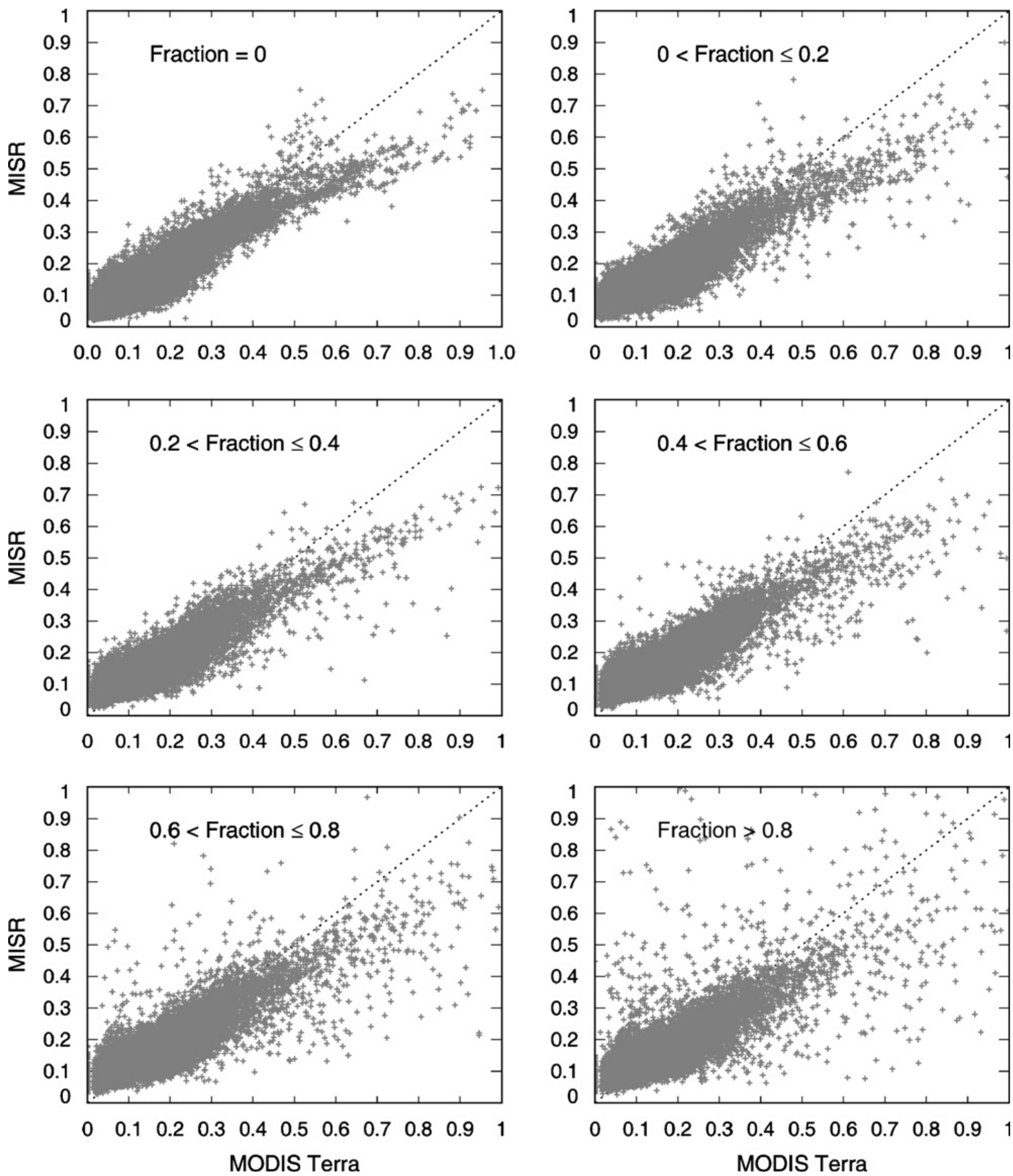

Fig. 2. MISR vs. MODIS AOTs at 550 nm over the oceans for six cloud fraction ranges: 0%, 0–20%, 20–40%, 40–60%, 60–80%, and 80–100%. The straight dotted lines depict the one-to-one perfect agreement.

0.882, 0.860, and 0.725 with the cloud fraction increasing from 0–20% to 80–100%. The goodness of the linear regression fit also deteriorates from $\mathrm{AOT_{MISR}} = 0.041+0.732 \times \mathrm{AOT_{MODIS}}$ for zero cloud fraction to $\mathrm{AOT_{MISR}} = 0.067+0.585 \times \mathrm{AOT_{MODIS}}$ for cloud fractions exceeding 80%. This is not surprising: as the cloud fraction increases, the aerosol retrievals can be expected to suffer progressively more from potential cloud contamination and 3D cloud illumination effects.

Fig. 3 parallels Fig. 1 and compares MODIS-Terra and MISR AEs. The MISR AE is calculated as a least-square linear fit to the logarithm of the AOTs evaluated at all four MISR wavelengths. The MODIS AE is computed using the 470 and 670 nm channels over the land and 550 and 860 nm channels over the oceans. Somewhat unexpectedly, both scatter plots show virtually no correlation between the MODIS and MISR AEs. Furthermore, one can see that the MODIS AEs retrieved over the land strongly cluster at values ~0.6–0.7 and ~1.6–1.8.

To further quantify the comparison shown in Fig. 1, we have evaluated the fractions of data points satisfying the following four criteria motivated by the published MODIS and MISR AOT retrieval accuracy claims:

$$\frac{|\mathrm{AOT_{MODIS}} - \mathrm{AOT_{MISR}}|}{\max(|\mathrm{AOT_{MODIS}}|, |\mathrm{AOT_{MISR}}|)} < 0.1 \text{ over ocean,} \tag{1}$$

$$|\mathrm{AOT_{MODIS}} - \mathrm{AOT_{MISR}}| < 0.03 \text{ over ocean,} \tag{2}$$

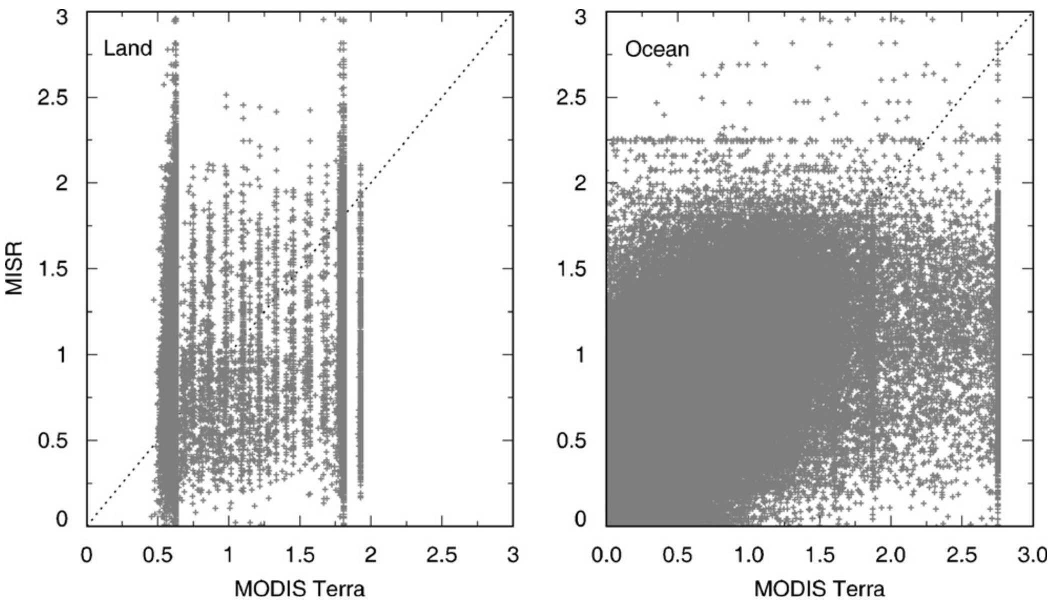

Fig. 3. MISR vs. MODIS-Terra AEs. The straight dotted lines depict the one-to-one perfect agreement.

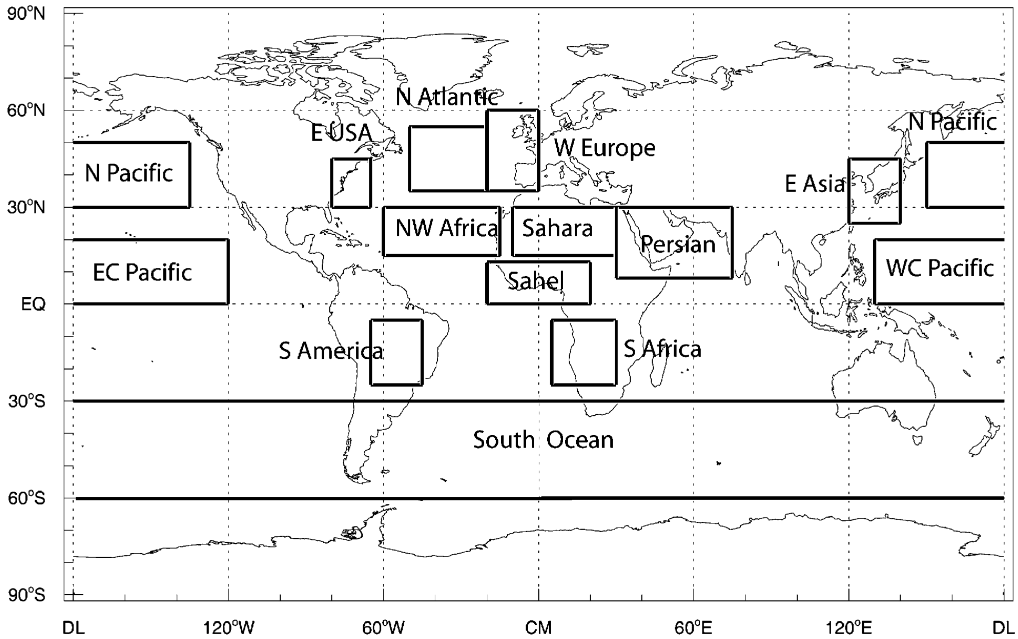

Fig. 4. Regions selected for MODIS–MISR AOT comparisons.

$$\frac{|\mathrm{AOT}_{\mathrm{MODIS}} - \mathrm{AOT}_{\mathrm{MISR}}|}{\max(|\mathrm{AOT}_{\mathrm{MODIS}}|, |\mathrm{AOT}_{\mathrm{MISR}}|)} < 0.15 \text{ over land,} \tag{3}$$

$$|\mathrm{AOT}_{\mathrm{MODIS}} - \mathrm{AOT}_{\mathrm{MISR}}| < 0.05 \text{ over land.} \tag{4}$$

We have found that the fractions of pixels satisfying criteria (1), (2), and either (1) or (2) over the oceans are 27.9%, 57.0%, and 57.3%, respectively. Over the land, the fractions of pixels satisfying criteria (3), (4), and either (3) or (4) are 12.3%, 28.2%, and 29.1%, respectively. These results demonstrate again that accurate radiometry-based AOT retrievals over the land are highly problematic.

3.2. Regional comparisons

To help identify regional AOT differences and correlate them with the expected predominant aerosol compositions, we have selected a number of specific geographic locations as shown in Fig. 4. These regions are believed to represent major aerosol types, e.g., dust over the Persian Gulf and the Sahara desert areas as well as off the west coast of Africa; biomass burning in

South America; biomass burning combined with the southward flow of mineral dust over the Sahel; sea salt aerosols over the South Ocean and Central Pacific areas; and regions affected by both natural and anthropogenic aerosol components with no single predominant aerosol species (Eastern United States, Western Europe, East Asia, North Atlantic, and North Pacific).

We compare separately AOT retrievals over water surfaces (Fig. 5) and over land areas (Fig. 6) whenever the specified regions contain both surface types, because both the MODIS and the MISR results are based on separate algorithms for performing retrievals over the oceans and over the land. One can see that although the MODIS–MISR agreement over the oceans is often worse than expected, in many cases it is acceptable (Fig. 5). However, the agreement over the land areas is often poor (Fig. 6).

Although the pixel-level MODIS and MISR results disagree considerably over the oceans, the differences in the corresponding regional averages turn out to be smaller than 0.004 in regions such as the Persian Gulf and South Ocean. In general, the comparison of regional AOT averages in Table 1 illustrates why it is so important to compare and analyze level 2 data. Interestingly, there are so many MODIS pixels over the land with negative or very small positive AOT values (the MODIS AOT look-up table range is between −0.1 and 5) that the average AOT is only 0.029 in the South American region, in contrast to the 0.139 MISR average. Furthermore, both the MODIS and the MISR AOT values over the land in such regions as Western Europe, East Asia, Eastern USA, and South America are surprisingly small and, in fact, are significantly smaller than those over the contiguous ocean areas. This likely indicates the failure of both algorithms to retrieve AOTs over the corresponding types of land surface.

3.3. Further analysis of global results

There are 745,068 collocated MODIS and MISR pixels for which the MODIS algorithm produced AOT results. Among them, 290,430 pixels have MISR aerosol retrievals and 454,638 pixels do not. The above analysis concerns the 290,430 pairs of coincident MODIS and MISR pixels that both have aerosol-retrieval results. However, the probability of not having

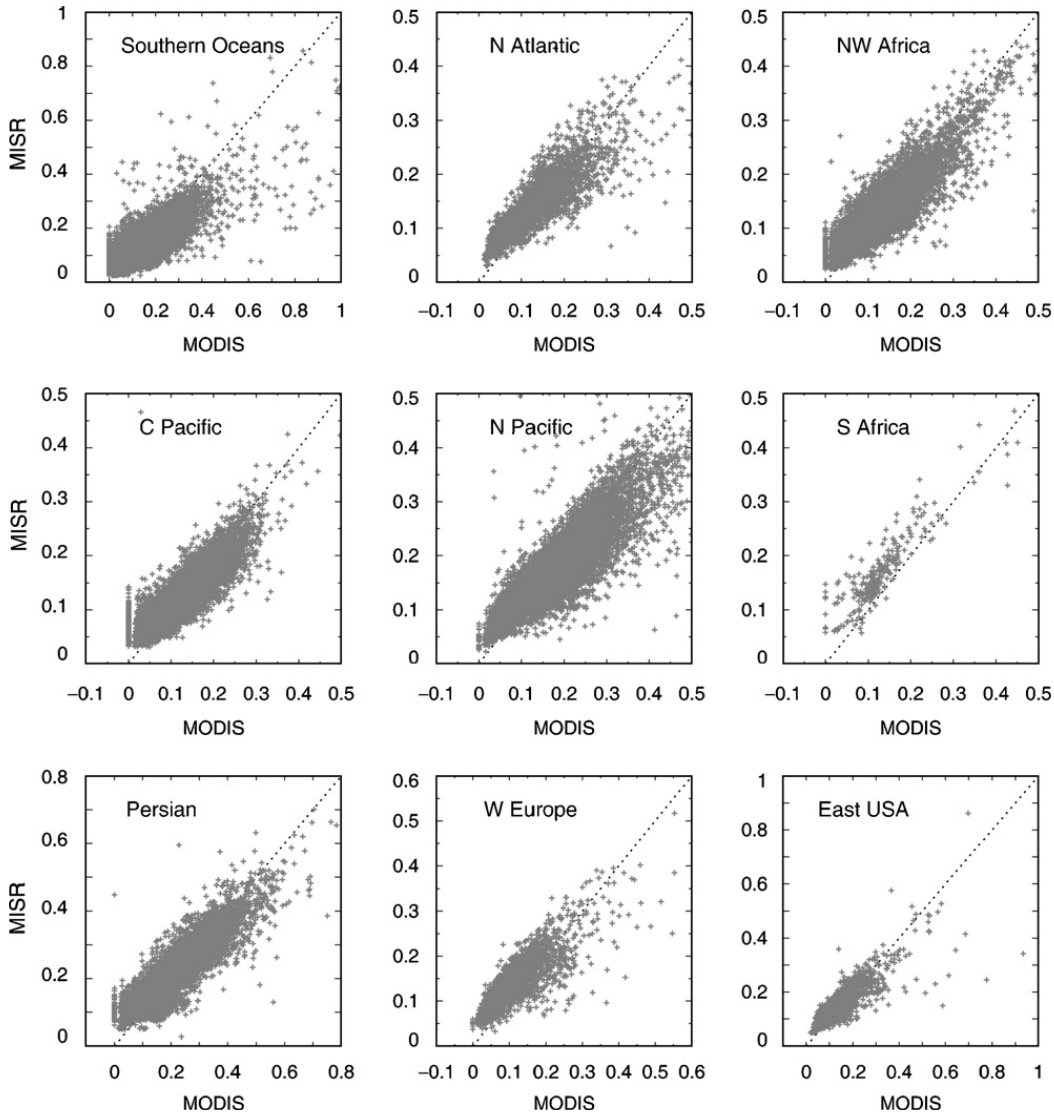

Fig. 5. Regional comparisons of collocated MODIS and MISR level 2 AOTs over ocean. The straight dotted lines depict the one-to-one perfect agreement.

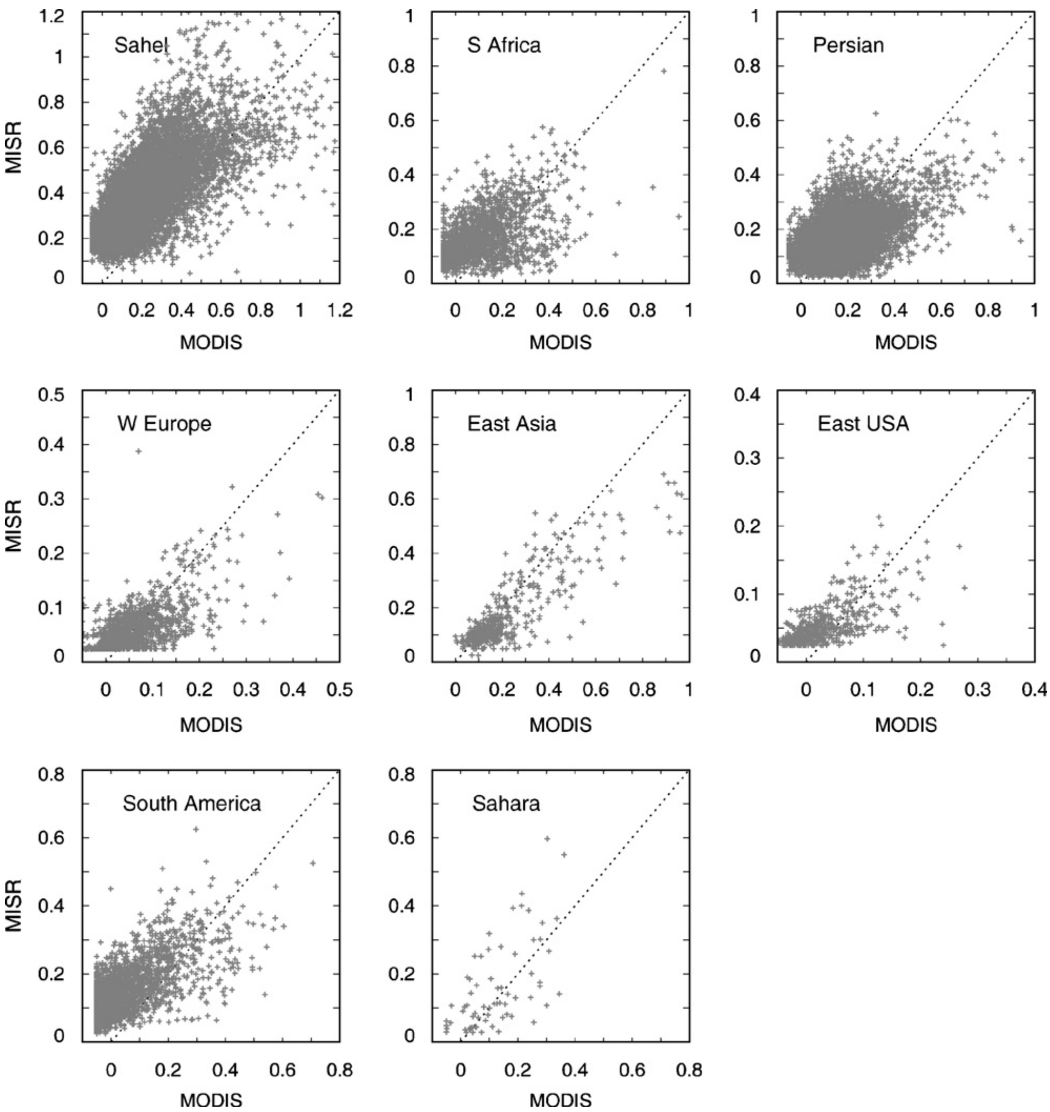

Fig. 6. Regional comparisons of collocated MODIS and MISR level 2 AOTs over land. The straight dotted lines depict the one-to-one perfect agreement.

Table 1
Regional AOT averages

Region	Over land		Over ocean	
	MODIS	MISR	MODIS	MISR
South Ocean	0.089	0.091	0.111	0.111
NW Africa	0.217	0.337	0.122	0.121
N. Atlantic	–	–	0.130	0.141
Central Pacific	0.137	0.121	0.116	0.112
N. Pacific	–	–	0.173	0.170
Sahel	0.233	0.405	0.556	0.431
S. Africa	0.113	0.172	0.127	0.168
Persian Gulf	0.188	0.182	0.204	0.208
W. Europe	0.062	0.064	0.108	0.132
E. Asia	0.225	0.178	0.263	0.240
E. USA	0.032	0.055	0.137	0.151
S. America	0.029	0.139	0.153	0.178
Sahara	0.124	0.159	–	–

a collocated MISR retrieval is significantly greater than the probability of having it: 61% as opposed to 39%. It is therefore important to analyze the reasons behind the lack of a MISR retrieval for a pixel which the MODIS retrieval algorithm considers suitable. Such information is available from the MISR product called SubregParamsAer (retrieval applicability mask). The dataset contains information on the retrieval status for each 1.1-km subregion for a given camera view (1–9) and spectral band (1–4). The fractional distribution of the reasons for not performing an aerosol retrieval is as follows:

0.1129	Clear
0.1318	Missing data
0.0007	Poor quality
0.0735	Glitter-contaminated
0.0037	Topography obscured
0.0000	Topography shadowed
0.0000	Topography complex
0.0216	Cloudy
0.0000	Cloud shadow
0.0885	Not smooth
0.1402	Not correlated
0.4111	Region not suitable
0.0065	Optically thick
0.0000	Too bright
0.0095	Fill value

The definitions of these categories can be found in the MISR "Level 2 Aerosol Retrieval Algorithm Theoretical Basis" document, Section 3.3.8 "Filter out unusable or contaminated subregions or channels" (http://eospso.gsfc.nasa.gov/eos_homepage/for_scientists/atbd/viewInstrument.php?instrument=19). Note that the MISR standard aerosol product reports AOTs on a 17.6-km grid. To make use of the information provided in the retrieval applicability mask, one must group all 16×16 1.1-km subregions into a 17.6 km pixel and then compute the corresponding statistics.

Of the pixels that the MODIS algorithm considers suitable, about 41% are considered by the MISR algorithm as unsuitable, 14% are discarded because of poor correlation of the equivalent reflectance spatial distribution from one view angle to another, and 13% are discarded because of missing data. There is an 11% probability that even a clear-sky pixel will be discarded, perhaps because at least one of the retrieved parameters happens to be out of its respective allowable range. In other words, because of the use of different retrieval approaches and because of different types of input radiance data, the MODIS and MISR algorithms quite often disagree over whether a pixel is even suitable for an aerosol retrieval. For example, the MISR multiangle capability can be used to impose an additional constraint such as the angle-to-angle correlation of the equivalent reflectances, which is something that the MODIS algorithm cannot have. This selection disagreement is only exacerbated by the frequent subsequent disagreements between the retrieved aerosol characteristics even for pixels considered suitable by both algorithms.

There is a total of 784,417 coincident MODIS and MISR pixels for which the MISR algorithm yielded an aerosol retrieval. Among them, there are only 285,699 pixels (or 36.4%) for which the MODIS algorithm yielded an aerosol retrieval, while the remaining 498,718 pixels (or 63.6%) have been rejected as unsuitable. Similar to MISR's retrieval applicability mask, but in a statistical fashion based on a 1-km subgrid retrieval status, the MODIS QA parameter (Quality_Assurance_Land and Quality_Assurance_Ocean; for description see http://modis-atmos.gsfc.nasa.gov/_docs/QA_Plan_2007_04_12.pdf) indicates the retrieval status for each level 2 grid. However, if there are multiple reasons for not making a retrieval in the designated pixel, the QA parameter reveals only one of them (L. Remer, personal communication).

The reasons as to why no MODIS inversion was performed for coincident pixels for which the MISR algorithm generated aerosol results are as follows.

Over land:

0.0539	No error
0.7091	Solar and observation angles out-of-bounds in look-up table
0.0000	Apparent reflectance out-of-bounds in look-up table
0.2370	Number of cloud and water-free pixels not met
0.0000	Thresholds of 2.1 μm not met
0.0000	Thresholds of 3.8 μm not met
0.0000	Thin cirrus detection not met

Over ocean:

0.0000	Retrieval is performed
0.8618	Glitter is present
0.1235	Cloudy
0.0000	R (0.865 μm) too low for retrieving optical thickness
0.0000	Total number of available VIS/SWIR wavelength bands (from 550 and 1240 nm) is insufficient
0.0000	Total number of available wavelengths <3
0.0147	Angles out-of-bounds
0.0000	Land present in 10×10 km box
0.0000	AOT (550 nm) <-0.01; algorithm found negative values of optical thickness (there is a problem)
0.0000	AOT (550 nm) $>$ 5.0; out-of-bounds in look-up table
0.0000	All channels do not have valid data

Thus over the oceans, the presence of a sun glint is the most important factor for the lack of a MODIS retrieval.

4. Conclusions

It follows from our analysis of coincident MODIS and MISR level 2 aerosol data that the collocated MODIS and MISR AOTs can substantially disagree both regionally and globally. It comes as no surprise that the agreement between the two datasets is better over the oceans than over the land. In this respect, it will be interesting to compare MISR retrievals over the land with the MODIS-based Deep Blue dataset [29]. Over water surfaces, the agreement improves under no-cloud or low-cloud conditions, with very few outliers, and worsens as the cloud fraction increases. There is essentially no correlation between the retrieved AEs. Thus our new results indicate that the significant discrepancies between the MODIS and MISR level 3 data identified in [13] cannot be attributed only to sampling effects.

Of the collocated pixels for which there is a MODIS aerosol retrieval, only $\sim$40% or fewer pixels have a MISR aerosol retrieval, and vice versa. This is mostly explained by the different characteristics of the MODIS and MISR observation strategies and the resulting differences in the corresponding retrieval algorithms. It was pointed out in [17] that MODIS and MISR retrieval areas over water surfaces frequently do not overlap since the MODIS observation direction can often be in the sun glint, whereas the MISR retrieval relies on the off-nadir cameras when the nadir view is glint-contaminated. This conclusion is obviously reinforced by our results. Also, in more than 40% of the cases MISR and MODIS disagreed over whether a region is suitable for aerosol retrieval. The cloud/no-cloud decisions made by the MODIS and MISR cloud screening procedures are not always the same. Quite often pixels were declared CLEAR by one algorithm but CLOUDY by the other. It is important to keep in mind that our analysis does not provide information on how often a scene is erroneously classified as either clear or cloudy by both algorithms simultaneously. This is an additional important source of aerosol-retrieval errors requiring a separate study [1,30].

Although our analysis reveals large MODIS–MISR differences in the retrieved aerosol parameters, it cannot be used to determine which algorithm yields a more accurate retrieval in each particular case or which algorithm is better in general. The reader may recall that a decade ago both instruments were planned to provide a dramatic improvement in the aerosol-retrieval capability from space. However, the identified differences between the MODIS and MISR level 2 results often significantly exceed the respective accuracy claims, which may indicate that neither instrument actually provides the expected improvement in a well-characterized and quantified way. Indeed, even when the MODIS and MISR retrieval algorithms make the same cloud/no-cloud decision for a scene and do perform an aerosol retrieval, there are often significant differences between the respective aerosol products caused by inherent differences in the sensitivity of MODIS and MISR radiances to the various parameters of the atmosphere–surface system. For example, the MISR instrument provides the multiangle observation capability important for identifying nonspherical aerosols [3,31–35] but cannot have adequate sensitivity to the presence of sub-visible cirrus clouds because of its limited spectral range. The absence of a meaningful correlation between the MODIS and MISR AEs likely indicates that the retrievals of the aerosol microphysics and number density with these radiometry-based instruments are highly unreliable [36]. Overall, these results demonstrate the urgency of flying a dedicated high-accuracy aerosol–cloud polarimeter such as the Aerosol Polarimetry Sensor [37].

Although we have explicitly presented comparison results for the month of January 2006, analogous comparisons of July 2006 MODIS and MISR retrievals lead to essentially the same conclusions. Thus our findings further illustrate the complexity of the problem of aerosol retrievals from satellite observations [13,19,37–40]. Unfortunately, they also imply that the creation of a unified MODIS–MISR aerosol climatology is likely to be a more nontrivial task than one might have expected, especially over the land.

Acknowledgments

We thank John Martonchik for valuable advice regarding the MISR aerosol-retrieval algorithm and datasets and Lorraine Remer for her assistance in the understanding of the MODIS aerosol product. Stimulating comments from two anonymous reviewers are also appreciated. This research was funded by the NASA Radiation Sciences Program managed by Hal Maring, by the NASA EOS program, and by the NASA Glory Mission project.

References

[1] Mishchenko MI, et al. Aerosol retrievals over the ocean by use of channels 1 and 2 AVHRR data: sensitivity analysis and preliminary results. Appl Opt 1999;38:7325–41.

[2] Geogdzhayev IV, et al. Global two-channel AVHRR retrievals of aerosol properties over the ocean for the period of NOAA-9 observations and preliminary retrievals using NOAA-7 and NOAA-11 data. J Atmos Sci 2002;59:262–78.

[3] Mishchenko MI, et al. Aerosol retrievals from AVHRR radiances: effects of particle nonsphericity and absorption and an updated long-term global climatology of aerosol properties. JQSRT 2003;79/80:953–72.

[4] Geogdzhayev IV, Mishchenko MI, Liu L, Remer L. Global two-channel AVHRR aerosol climatology: effects of stratospheric aerosols and preliminary comparisons with MODIS and MISR retrievals. JQSRT 2004;88:47–59.

[5] Geogdzhayev IV, et al. Regional Advanced Very High Resolution Radiometer-derived climatology of aerosol optical thickness and size. J Geophys Res 2005;110:D23205.

[6] Mishchenko MI, et al. Long-term satellite record reveals likely recent aerosol trend. Science 2007;315:1543.

[7] Mishchenko MI, Geogdzhayev IV. Satellite remote sensing reveals regional tropospheric aerosol trends. Opt Express 2007;15:7423–38.

[8] George JP, Harenduprakash L, Mohan M. Multi year changes of aerosol optical depth in the monsoon region of the Indian Ocean since 1986 as seen in the AVHRR and TOMS data. Ann Geophys 2008;26:7–11.
[9] Liu L, et al. Global validation of two-channel AVHRR aerosol optical thickness retrievals over the oceans. JQSRT 2004;88:97–109.
[10] Smirnov A, et al. Ship-based aerosol optical depth measurements in the Atlantic Ocean: comparison with satellite retrievals and GOCART model. Geophys Res Lett 2006;33:L14817.
[11] Stowe LL, et al. The Advanced Very High Resolution Radiometer (AVHRR) Pathfinder Atmosphere (PATMOS) climate dataset: initial analyses and evaluations. J Clim 2002;15:1243–60.
[12] Zhao TX-P, et al. Study of long-term trend in aerosol optical thickness observed from operational AVHRR satellite instrument. J Geophys Res 2008;113:D07201.
[13] Mishchenko MI, et al. Past, present, and future of global aerosol climatologies derived from satellite observations: a perspective. JQSRT 2007;106:325–47.
[14] Abdou W, et al. Comparison of coincident Multiangle Imaging Spectroradiometer and Moderate Resolution Imaging Spectroradiometer aerosol optical depths over land and ocean scenes containing Aerosol Robotic Network sites. J Geophys Res 2005;110:D10S07.
[15] Myhre G, et al. Intercomparison of satellite retrieved aerosol optical depth over ocean during the period September 1997 to December 2000. Atmos Chem Phys 2005;5:1697–719.
[16] Liu L, et al. Assessing Goddard Institute for Space Studies ModelE aerosol climatology using satellite and ground-based measurements: a comparison study. J Geophys Res 2006;111:D20212.
[17] Kahn R, et al. Satellite-derived aerosol optical depth over dark water from MISR and MODIS: comparisons with AERONET and implications for climatological studies. J Geophys Res 2007;112:D18205.
[18] Kokhanovsky AA. Aerosol optics. Berlin: Springer; 2008.
[19] Mishchenko MI, et al. Monitoring of aerosol forcing of climate from space: analysis of measurement requirements. JQSRT 2004;88:149–61.
[20] Zhao TX-P, et al. Derivation of component aerosol direct radiative forcing at the top of atmosphere for clear-sky oceans. JQSRT 2008;109:1162–86.
[21] Xiong X, Che N, Barnes W. Terra MODIS on-orbit spatial characterization and performance. IEEE Trans Geosci Remote Sens 2005;43:355–65.
[22] Tanré D, Kaufman YJ, Herman M, Mattoo S. Remote sensing of aerosol properties over oceans using the MODIS/EOS spectral radiances. J Geophys Res 1997;102:16,971–88.
[23] Levy RC, et al. Evaluation of the Moderate-Resolution Imaging Spectroradiometer (MODIS) retrievals of dust aerosol over the ocean during PRIDE. J Geophys Res 2003;108:8594.
[24] Remer LA, et al. The MODIS aerosol algorithm, products, and validation. J Atmos Sci 2005;62:947–73.
[25] Kahn R, et al. MISR calibration and implications for low-light-level aerosol retrieval over dark water. J Atmos Sci 2005;62:1032–52.
[26] Martonchik JV, et al. Techniques for the retrieval of aerosol properties over land and ocean using multiangle imaging. IEEE Trans Geosci Remote Sens 1998;36:1212–27.
[27] Martonchik JV, Diner DJ, Crean KA, Bull MA. Regional aerosol retrieval results from MISR. IEEE Trans Geosci Remote Sens 2002;40:1520–31.
[28] Kahn R, et al. Multiangle Imaging Spectroradiometer (MISR) global aerosol optical depth validation based on 2 years of coincident Aerosol Robotic Network (AERONET) observation. J Geophys Res 2005;110:D10S04.
[29] Hsu NC, Tsay SC, King MD, Herman JR. Aerosol properties over bright-reflecting source regions. IEEE Trans Geosci Remote Sens 2004;42:557–69.
[30] Martins JV, et al. MODIS cloud screening for remote sensing of aerosols over oceans using spatial variability. Geophys Res Lett 2002;29.
[31] Mishchenko MI, Travis LD, Kahn RA, West RA. Modeling phase functions for dustlike tropospheric aerosols using a shape mixture of randomly oriented polydisperse spheroids. J Geophys Res 1997;102:16831–47.
[32] Zhao TX-P, et al. A study of the effect of non-spherical dust particles on the AVHRR aerosol optical thickness retrievals. Geophys Res Lett 2003;30:1317.
[33] Dubovik O, et al. The application of spheroid models to account for aerosol particle non-sphericity in remote sensing of desert dust. J Geophys Res 2006;111:D11208.
[34] Nousiainen T, Kahnert M, Veihelmann B. Light scattering modeling of small feldspar aerosol particles using polyhedral prisms and spheroids. JQSRT 2006;101:471–87.
[35] Horvath H, Kasahara M, Tohno S, Kocifaj M. Angular scattering of the Gobi Desert aerosol and its influence on radiative forcing. J Aerosol Sci 2006;37:1287–302.
[36] Mishchenko MI, et al. Retrieving CCN column density from single-channel measurements of reflected sunlight over the ocean: a sensitivity study. Geophys Res Lett 1997;24:2655–8.
[37] Mishchenko MI, et al. Accurate monitoring of terrestrial aerosols and total solar irradiance: introducing the Glory Mission. Bull Am Meteorol Soc 2007;88:677–91.
[38] King MD, Kaufman YJ, Tanré D, Nakajima T. Remote sensing of tropospheric aerosols from space: past, present, and future. Bull Am Meteorol Soc 1999;80:2229–59.
[39] Chowdhary J, Cairns B, Mishchenko M, Travis L. Retrieval of aerosol properties over the ocean using multispectral and multiangle photopolarimetric measurements from the Research Scanning Polarimeter. Geophys Res Lett 2001;28:243–6.
[40] Hasekamp O, Landgraf J. Retrieval of aerosol properties over land surfaces: capabilities of multiple-viewing-angle intensity and polarization measurements. Appl Opt 2007;46:3332–44.